

Unveiling the Power of Mixup for Stronger Classifiers

Zicheng Liu*,¹² Siyuan Li*,¹² Di Wu,¹² Zhiyuan Chen,¹ Lirong Wu,¹² Jianzhu Guo,³ Stan Z. Li,¹²

¹AI Lab, School of Engineering, Westlake University, Hangzhou, Zhejiang, China

²Institute of Advanced Technology, Westlake Institute for Advanced Study, Hangzhou, Zhejiang, China

³CBSR & NLPR, Institute of Automation, Chinese Academy of Sciences, Beijing, China

{liuzicheng, lisiyuan, wudi, chen zhiyuan, wulirong, Stan.ZQ.Li}@westlake.edu.cn, guojianzhu1994@gmail.com

Abstract

Mixup-based data augmentations have achieved great success as regularizers for deep neural networks. However, existing methods rely on deliberately handcrafted mixup policies, which ignore or oversell the semantic matching between mixed samples and labels. Driven by their prior assumptions, early methods attempt to smooth decision boundaries by random linear interpolation while others focus on maximizing class-related information via offline saliency optimization. As a result, the issue of label mismatch has not been well addressed. Additionally, the optimization stability of mixup training is constantly troubled by the label mismatch. To address these challenges, we first reformulate mixup for supervised classification as two sub-tasks, mixup sample generation and classification, then propose *Automatic Mixup* (AutoMix), a revolutionary mixup framework. Specifically, a learnable lightweight Mix Block (MB) with a cross-attention mechanism is proposed to generate a mixed sample by modeling a fair relationship between the pair of samples under direct supervision of the corresponding mixed label. Moreover, the proposed Momentum Pipeline (MP) enhances training stability and accelerates convergence on top of making the Mix Block fully trained end-to-end. Extensive experiments on five popular classification benchmarks show that the proposed approach consistently outperforms leading methods by a large margin.

1 Introduction

Recent years have witnessed great success of Deep Neural Networks (DNNs) in various tasks, such as object recognition (He et al. 2016; Lin et al. 2017), semantic segmentation (Ren et al. 2015; Chen et al. 2017; Ronneberger, Fischer, and Brox 2015), natural language processing (Devlin et al. 2018), and reinforcement learning (Silver et al. 2016). Most of these successes can be attributed to the use of complex network architectures with numerous parameters and a sufficient amount of data. However, in the case of insufficient data, models with high complexity are prone to suffer from overfitting and overconfidence, resulting in poor performance and generalization abilities (Srivastava et al. 2014). Moreover, this problem may be further worsened for samples with batch effects (Ben-David et al. 2010).

*These authors contributed equally.

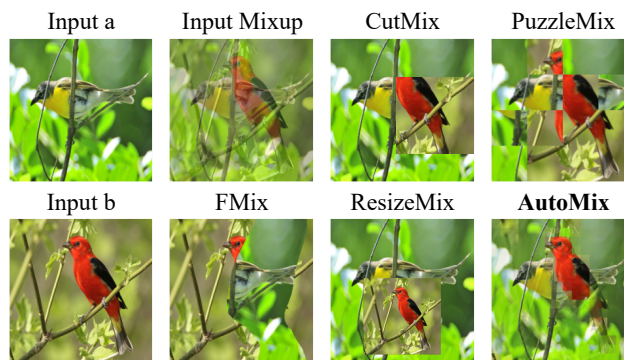


Figure 1: Visualization comparison of mixup methods. AutoMix generates mixed samples by a mask learned from the feature map rather than predefined policies.

To improve the generalization ability of DNNs, a series of researches have been proposed to design regularizers or to augment the data with task-dependent techniques (Bishop 2006). Recently, a task-dependent augmentation strategy, named MixUp (Zhang et al. 2017), is proposed to increase the data diversity via convex combination. CutMix (Yun et al. 2019) designs a patch replacement strategy that randomly replaces a patch from two images. Several types of research (Baek, Bang, and Shim 2021; Faramarzi et al. 2020) improve CutMix (Yun et al. 2019), while the proposed cutting strategies cannot guarantee that the mixed sample contains target objects which might cause the *label mismatch* problem. The saliency-based mixup methods which aim to solve this problem go to another extreme: maximizing the saliency region to confirm the co-presence of the targets in the mixed samples. Although SaliencyMix (Uddin et al. 2020) and PuzzleMix (Kim, Choo, and Song 2020) introduce more precise mixing policies based on class-related saliency information, a complete target should correspond to a complete label, not an unbalanced mixed label. Evidently, it is not successful modeling that the mixup policies are transformed from a random linear interpolation to an offline saliency optimization. Overall, previous offline methods were incapable of accurately modeling balanced semantic relationships between the mixed data pairs and labels.

So, what is the accurate relationship between mixed sample and label, and how to stabilize the mixup train-

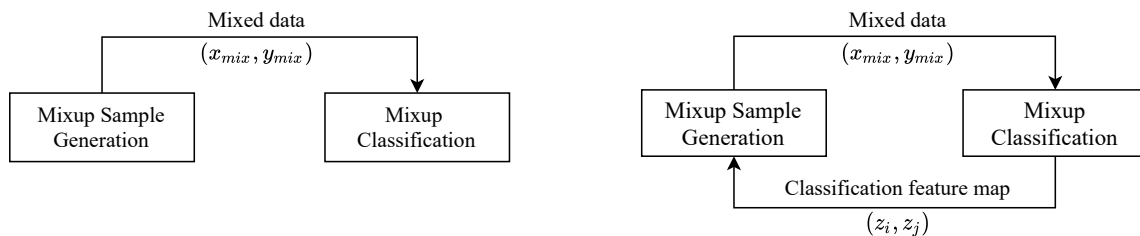


Figure 2: The difference between AutoMix and offline approaches. **Left:** Offline mixup methods, where a fixed mixup policy generates mixed samples for the classifier to learn from. **Right:** AutoMix, where the mixup policy is trained with the feature map.

ing? To answer these two questions, we reformulate the mixup training into two sub-tasks, mixed sample generation, and classification. We regard mixed sample generation as an auxiliary task for classification. Based on the reformulation, we propose a novel mixup framework called AutoMix. In contrast to the offline generation, AutoMix automatically generates mixed samples by employing a cross-attention mechanism based Mix Block (MB) module which is optimized end-to-end in collaboration with the Momentum Pipeline (MP). The proposed MB module is designed for modeling the proportional relation of samples utilizing their feature maps and mixed labels. Additionally, MP can also make MB fully trainable on top of alleviating the *optimization instability* via optimizing both the mixed samples generation and classification tasks in a unified framework. Comprehensive experiments on five classification benchmarks, including CIFAR-10/100, Tiny-ImageNet, ImageNet, and CUB-200, show that our AutoMix consistently outperforms existing mixup methods. We further provide an extensive analysis of the proposed components and hyper-parameter settings. Our main contributions are summarized as follows:

- From a fresh perspective, we divide the mixup training into two subtasks: mixed sample generation and classification, and regard the generation as an auxiliary task to the classification. We unified them into a framework named AutoMix to optimize the sample mixup policy online.
- To tackle *label mismatch* and *optimization instability* problems involved with mixup, we propose Mix Block and Momentum Pipeline, which optimizes the two sub-tasks online to learn proportional semantic relationships and improves mixup training stability.
- AutoMix surpasses counterparts significantly on classification and downstream tasks, as demonstrated in extensive experiments. Moreover, AutoMix nearly doubles the training efficiency compared to saliency-based methods.

2 Related Work

Mixup(Zhang et al. 2017), the first mixing-based data augmentation algorithm, was proposed to generate mixed samples with mixed labels by convex interpolations (e.g., linear interpolation) of any two samples and their unique one-hot labels. ManifoldMix (Verma et al. 2019) extends the Mixup from the input space to the hidden space of DNNs. CutMix (Yun et al. 2019) incorporates the Dropout strategy into the mixup strategy, and proposes a mixing strategy based on the patch of the image, i.e., randomly replacing a local rectangular

area in images. Based on CutMix, ResizeMix (Qin et al. 2020) replaces one complete image directly into a local rectangular area of another image after scaling down to maintain the information integrity. SaliencyMix (Uddin et al. 2020), on the other hand, obtains saliency regions in the image based on a universal saliency detector and blends them to obtain more relevant mixed samples with labels. Furthermore, PuzzleMix (Kim, Choo, and Song 2020), and Co-Mixup (Kim et al. 2021) propose offline strategies to find optimal mixup masks by maximizing the saliency information. FMix (Harris et al. 2020) transforms the image into Fourier space (spectrum domain) to generate binary masks by setting a threshold. Compared with existing algorithms, our approach does not use a sample mixing strategy designed manually based on a priori knowledge or saliency information but instead adaptively generates mixed samples based on mixing ratios and the feature maps in an end-to-end fashion.

3 Preliminaries

Mixup training. We first consider the general image classification task with k different classes: given a set of n samples $X = \{x_1, x_2, \dots, x_n\} \in \mathbb{R}^{n \times W \times H \times C}$ and their ground-truth class labels $Y = \{y_1, y_2, \dots, y_n\} \in \mathbb{R}^{n \times k}$, encoded by a one-hot vector $y_i \in \mathbb{R}^k$. We seek the mapping from the data x to its class label y modeled by a deep network $f_\theta : x \mapsto y$ with network parameters $\theta \in \Theta$ by optimizing a classification loss $\ell(\cdot)$, say the cross entropy loss (CE),

$$\min_{\theta} \ell_{CE}(f_\theta(x), y). \quad (1)$$

Then we consider the mixup classification task: given a sample mixup function h , a label mixup function g , and a mixing ratio λ sampled from $Beta(\alpha, \alpha)$ distribution, we can generate the mixup data X_{mix} with $x_{mix} = h(x_i, x_j, \lambda)$ and the mixup label Y_{mix} with $y_{mix} = g(y_i, y_j, \lambda)$. Similarly, we find $f_\theta : x_{mix} \mapsto y_{mix}$ by optimizing $\ell_{MCE}, \lambda CE(x_i, y_i) + (1 - \lambda)CE(x_j, y_j)$,

$$\min_{\theta} \ell_{MCE}(f_\theta(h(x_i, x_j, \lambda)), g(y_i, y_j, \lambda)). \quad (2)$$

Reformulation: generation and classification. Comparing Eq.1 and Eq.2, the mixup training has the following features: (1) extra mixup functions, g and h , are required to generate X_{mix} and Y_{mix} . (2) the classification performance of f_θ depends on X_{mix} and Y_{mix} . Naturally, from a novel view, we can split the mixup task into two complementary sub-tasks: (i) mixed sample generation and (ii) mixup classification. Notice that the sub-task (i) is subordinate to (ii) because the

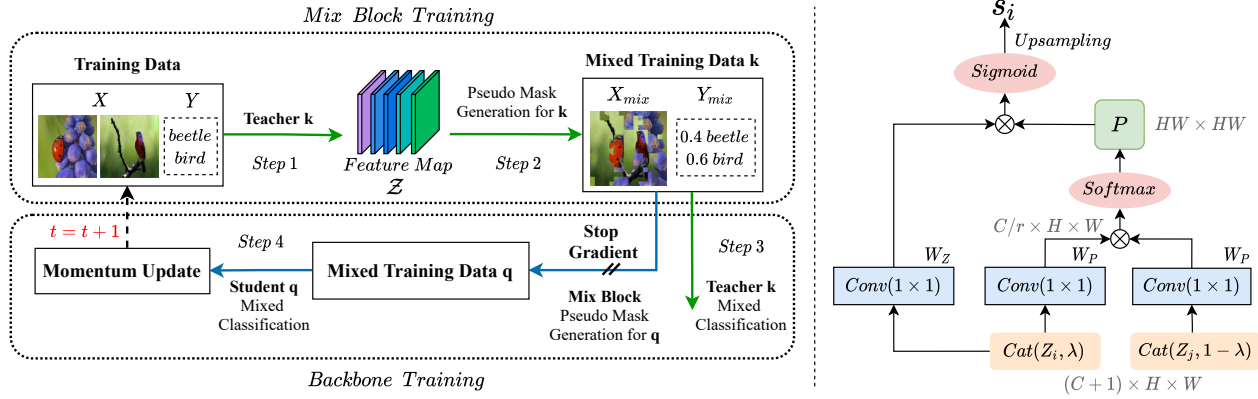


Figure 3: Overview of the AutoMix. The **left** diagram represents the proposed algorithm flow chart. The blue and green lines indicate the classifier training and the mix block training, correspondingly. The **right** diagram is the architecture of Mix Block.

final goal is to obtain a stronger classifier. Therefore, in this reformulated mixup framework, we regard (i) as an auxiliary task for the classification task. Since g is usually designed as a linear interpolation, i.e., $g(y_i, y_j) = \lambda y_i + (1 - \lambda)y_j$, h becomes the key function to determine the performance of the model. Generalizing offline methods, we define a parametric mixup function h_ϕ as the sub-task with another set of parameters $\phi \in \Phi$. To differentiate the function of losses, cls denotes classification task and gen denotes generation task:

$$\min_{\theta, \phi} \ell_{MCE}^{cls}(f_\theta(\ell^{gen}(h_\phi(x_i, x_j, \lambda))), g(y_i, y_j, \lambda)). \quad (3)$$

Offline mixup limits the power of mixup. Ideally, optimal h_ϕ is the inverse mapping of the mixup classification task, which generates mixed sample by $x_{mix} = h_\phi^*(x_i, x_j, \lambda) = f_\theta^{-1}(x_i, x_j, \lambda)$. However, it is hard to find optimal h_ϕ fits f_θ^{-1} perfectly because the mixup data X_{mix} cannot be sampled in reality. Hence, the previous methods focus on manually designing h_ϕ in an offline and nonparametric manner based on their prior hypotheses. As mentioned in Sec.1, they gradually convert h from a simple linear interpolation to an optimization algorithm with the goal of maximizing saliency information, based on their assumptions of smoothing classification boundaries and target co-presence. Nevertheless, in comparison to linear mixup methods, the improved idea of saliency-based methods requires extra computation and introduces the *label mismatch* issue, while the *optimization instability* remains unsolved. The main reason is that they build an indirect connection between the two sub-tasks, as shown in the left of Fig.2. Thus, *combining these two sub-tasks in a mutually beneficial manner is mixup truly needed.*

4 AutoMix

We build the bridge between the mixup generation and classification task with a unified optimization framework named as AutoMix. An comparison overview with offline approaches is presented in Fig.2. The main difference is that AutoMix makes generation task can be directly optimized under the same loss ℓ_{MCE} online and serves for classification task, whose generated mixed samples are complementary. Two obstacles are addressed in this framework, *label mismatch*

and *optimization instability*, by proposed Mix Block (MB) and Momentum Pipeline (MP), respectively. The schematic of AutoMix is illustrated in Fig.3.

4.1 Label Mismatch: Mix Block

We have examined that offline approaches are incapable of addressing the *label mismatch* issue in mixup training. This paper presents a novel module named Mix Block (MB) \mathcal{M}_ϕ for learning an online mixup policy without requiring extensive saliency computation. MB generate a pixel-wise mixup mask $s \in \mathbb{R}^{H \times W}$ for the input image, where $s_{w,h} \in [0, 1]$. The core of MB is the devised lambda embedded cross-attention mechanism, which is used to represent the pixel-level proportional relationships between a given data pair by taking advantage of the spatial sparsity and rich semantic information in deep features of CNN networks. Thus, the feature map z from the backbone f_θ is utilized to connect the two sub-tasks of mixup. Additionally, to facilitate the capture of class-related information in the generated mixed samples, the MB training is directly supervised by the mixup classification loss ℓ_{MCE} in an end-to-end manner.

Cross-attention mechanism Intuitively, the generation task is formulated as a regression problem: given a sample pair (x_i, x_j) and a mixup ratio λ , MB predicts the probability that each pixel on x_{mix} belongs to x_i based on the feature map pair (z_i, z_j) and λ . As shown in Fig.3, we combine λ with the l -th feature map in a simple and efficient way by concatenating, $z_\lambda^l = \text{concat}(z, \lambda)$. Then we calculate the global pixel-level cross-attention between λ embedded $z_{i,\lambda}^l$ and $z_{j,1-\lambda}^l$ to get the similarity matrix P ,

$$P(z_{i,\lambda}^l, z_{j,1-\lambda}^l) = \text{Softmax}\left(\frac{W_P z_{i,\lambda}^l \otimes W_P z_{j,1-\lambda}^l}{C(z_{i,\lambda}^l, z_{j,1-\lambda}^l)}\right), \quad (4)$$

where W_P denotes a shared linear transformation matrices (e.g., 1×1 convolution), \otimes denotes matrix multiplication, and $C(z_{i,\lambda}^l, z_{j,1-\lambda}^l)$ is a normalization factor. Notice that $P(z_{i,\lambda}^l, z_{j,1-\lambda}^l)$ is the normalized pairwise similarity matrix between every spatial position on $z_{i,\lambda}^l$ and $z_{j,1-\lambda}^l$. Then, we



Figure 4: AutoMix samples with changing mixing ratio λ .

can compute the mixup mask s_i for $z_{i,\lambda}^l$ as

$$s_i = U(\text{Sigmoid}(P(z_{i,\lambda}^l, z_{j,1-\lambda}^l)) \otimes W_Z z_{i,\lambda}^l), \quad (5)$$

where U is an upsampling operation; s_i devotes a $H \times W$ tensor where each coordinate indicates the probability of choosing pixels in x_i after mixup. We can also compute s_j symmetrically with the same process and transposed similarity matrix P^T . Notice that a nearest upsampling function is adopted as U . To force MB taking the given λ into account, we align the mean of the mask to λ with a small margin ϵ ,

$$\mathcal{L}_{mask} = \gamma \max\left(\left|\lambda - \frac{1}{HW} \sum_{h,w} s_{i,h,w}\right| - \epsilon, 0\right), \quad (6)$$

where γ is a loss weight linearly decreased to 0 during training. We set the initial γ to 0.1 and $\epsilon = 0.1$. As for inference, \mathcal{M}_ϕ is able to generate a pair of mask (s_i, s_j) adaptively according to the feature pair (z_i, z_j) and the ratio λ with the λ embedded cross-attention mechanism, where $s_j = 1 - s_i$.

Mixup in end-to-end training Given a set of labeled data $\mathcal{D} = \{(x_i, y_i)\}_{i=1}^{n_D}$ and the corresponding feature map $\mathcal{Z} = \{z_1, z_2, \dots, z_n\}$. Intuitively, we can simply replace the $\mathcal{M}_\phi(\cdot)$ with scalar λ to attain the vanilla version of mixup (Zhang et al. 2017). Formally, for each data pair $((x_i, y_i), (x_j, y_j))$ in \mathcal{D} and their λ embedded feature map $(z_{i,\lambda}^l, z_{j,1-\lambda}^l)$, our mixup policy h_ϕ is summarized as

$$h_\phi(x_i, x_j) = (1 - \mathcal{M}_\phi(z_{i,\lambda}^l, z_{j,1-\lambda}^l)) \odot x_i + \mathcal{M}_\phi(z_{i,\lambda}^l, z_{j,1-\lambda}^l) \odot x_j, \quad (7)$$

where \odot denotes element-wise product. Notice that AutoMix uses standard cross-entropy loss ℓ_{CE} as default. ℓ_{CE} loss facilitates the backbone to learn discriminative feature map at the early stage so that speedups MB converges. Thus, the whole model is optimized end-to-end with a joint loss:

$$\mathcal{L}(\theta, \phi) = \ell_{CE} + \ell_{MCE} + \mathcal{L}_{mask}. \quad (8)$$

Further, since MB itself can be trained online with backbone via ℓ_{MCE} , *no additional computational overhead to maximize the saliency region*. Ablation studies also confirm that AutoMix achieves higher performance and requires less training time than saliency-based methods.

4.2 Optimization Instability: Momentum Pipeline

Recall the *optimization instability* problem in mixup training: the intervention of virtual mixed samples causes training

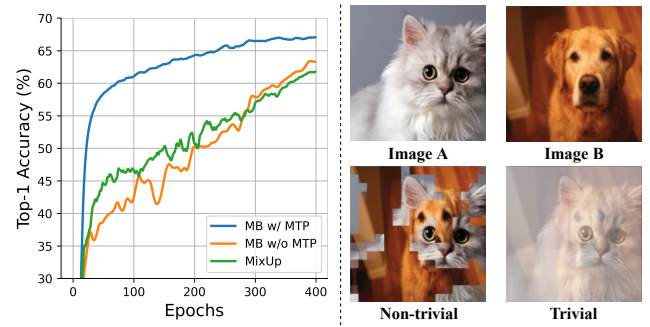


Figure 5: Training accuracy plot and illustration of different solutions of mixed sample. MP stabilizes mixup training and mitigates the trivial solution problem of MB.

oscillation. Experiments demonstrate that the oscillation problem could cause MB to fall into trivial solution (degraded to MixUp., illustrated in Fig.5) if \mathcal{M}_ϕ is optimized with f_θ without any constraints. Explained intuitively, due to the optimization of ϕ is affected by θ under the supervision of the same loss ℓ_{MCE} , an unstable training process and feature output cannot ensure that the training of MB proceeds appropriately. Formally, according to Eq.3 and Eq.8, for each iteration, the gradient for MB of \mathcal{L}^{cls} can be formulated as

$$\nabla_\phi \mathcal{L}^{cls} \propto \nabla_\phi h_\phi(x_i, x_j, \lambda) \odot f'_\theta(h_\phi(x_i, x_j, \lambda)). \quad (9)$$

It is notable that the instability of f_θ may result in a vicious cycle of the joint training. As a consequence, the primary goal of getting the Eq.(3) operating well is to ensure that f_θ outputs stable features and, to the extent possible, that ϕ and θ can focus on their own tasks in the case of using the same loss. Inspired by methods in self-supervised learning (He et al. 2020; Grill et al. 2020), they adopted momentum pipeline (MP) to avoid the feature collapse and realized that the teacher network f_k of the Siamese network shows more stable performance than student network f_q . Along this path, we designed a new MP for decoupling the nested optimization problem of Automix: the student network f_q focuses on classification task, while the stable teacher network f_k is connected with MB to perform generation task. Moreover, optimizing Eq.8 with batch approach requires X_{mix} generated by f_k and \mathcal{M}_ϕ first and then using X_{mix} to optimize f_q . By analogy, referring to the Expectation-Maximization (EM) algorithm, the two sets of parameters θ and ϕ can be optimized in alternating way by the designed MP, i.e., first fix one set of parameters to optimize the other. Formally, we can optimize both θ and ϕ by solving the following equations:

$$\theta_q^t \leftarrow \underset{\theta}{\operatorname{argmin}} \mathcal{L}(\theta_q^{t-1}, \phi^{t-1}), \quad (10)$$

$$\phi^t \leftarrow \underset{\phi}{\operatorname{argmin}} \mathcal{L}(\theta_k^t, \phi^{t-1}), \quad (11)$$

where t is the iteration step, θ_q and θ_k represent the parameters of student and teacher network, respectively. Note that f_q and f_k share the same network structure but the parameters of f_k are updated via a momentum rule from f_q :

$$\theta_k \leftarrow r(m)\theta_k + (1 - r(m))\theta_q, \quad (12)$$

where $m \in [0, 1)$ is the momentum decay coefficient, and $r(\cdot)$ is the scheduler function, which adjust m in a predefined pattern. It is worthy to mention that *MP not only solves optimization instability, but also significantly speeds training convergence*. Ablation studies and experiments results in Tab.6 and Fig.5 also demonstrate the high efficiency of MP.

5 Experiments

We evaluate AutoMix in three dimensions: (1) Image classification in various scenarios, (2) Robustness against corruption, and (3) Localization with weak supervision. All experiments are conducted with PyTorch and Tesla V100 GPU.

5.1 Evaluation on Image Classification

This subsection demonstrates the performance gain of AutoMix for various image classification tasks on five image benchmarks, including CIFAR-10/100 (Krizhevsky, Hinton et al. 2009), Tiny ImageNet (Chrabaszcz, Loshchilov, and Hutter 2017), ImageNet-k (Russakovsky et al. 2015) and CUB-200 (Wah et al. 2011). To verify the generalizability of AutoMix for different scale network architectures, the experiments use residual neural networks ResNet (R) and ResNeXt (32x4d) (RX) (Xie et al. 2017) as backbone networks. Also, all experiments use Cosine Scheduler (Loshchilov and Hutter 2016) to adjust the learning rate, and SGD as optimizer. For a fair comparison, grid search is performed for several common hyper-parameters of all mixup methods, including $\alpha \in \{0.2, 0.5, 1, 2, 4\}$ and cosine scheduler $lr_{min} \in \{5e-2, 1e-2, 5e-3, 1e-3, 1e-4, 0\}$, then we use $\alpha = 1$ and $lr_{min} = 0$ by default; the rest of the hyper-parameters are set the same as the original paper. Specifically, the momentum decay coefficient m start from $m \in \{0.999, 0.996\}$ and is gradually increased to 1 in a cosine curve. We report the results of optimal feature layer among $l \in \{1, 2, 3, 4\}$ on each dataset, using l_3 by default. For all experiments, we report the *mean of 3 trials* where the *median* of performances in the last 10 training epochs is recorded for each trial.

CIFAR Datasets

Settings. RandomFlip and RandomCrop with 4 pixels padding to zero are used as the base data augmentation techniques. On CIFAR dataset, the following hyper-parameters were set identically for all algorithms. SGD weight decay parameter is set to 0.0001, momentum is set to 0.9, initial learning rate is 0.1, and train 800 epochs with the Batch size of 100. Except AutoMix, the rest of mixup algorithms

use $lr_{min} = 0$. Only $\alpha = 2$ is used for ManifoldMix and AutoMix, while the rest of algorithms uses $\alpha = 1$.

Classification. The classification performance on CIFAR-10/100 dataset is shown in Tab.1. We can observe that AutoMix achieves competitive results and outperforms other algorithms. Moreover, AutoMix performs even better on more challenging CIFAR-100. In particular, on CIFAR-10, AutoMix surpasses the previous best algorithm 0.3% and 0.71% on ResNet-18 (R-18) and ResNeXt-50 (RX-50) respectively. On CIFAR-100, the margin rises to 1.79% and 0.76%, correspondingly. On CIFAR-100, it is noteworthy that AutoMix performs better on more challenging tasks and this is also verified on Imagenet experiments.

Method	CIFAR-10		CIFAR-100		CUB-200	
	R-18	RX-50	R-18	RX-50	R-18	RX-50
Vanilla	95.50	96.23	78.04	81.09	77.68	83.01
MixUp	96.62	97.30	79.12	82.10	78.39	84.58
CutMix	96.68	97.01	78.17	78.32	78.40	85.68
ManifoldMix	96.71	97.33	80.35	82.88	79.76	86.38
SaliencyMix	96.53	97.18	79.12	78.77	77.95	83.29
FMix	96.58	96.76	79.69	79.02	77.28	84.06
PuzzleMix	97.10	97.27	80.43	82.57	78.63	84.51
ResizeMix	96.76	97.21	80.01	79.73	78.50	84.77
AutoMix (ours)	97.40	98.04	82.04	83.64	79.87	86.56
Gain	+0.30	+0.71	+1.66	+0.76	+0.11	+0.18

Table 1: Top-1 accuracy of various algorithms based on ResNet-18 and ResNeXt-50 on CIFAR and CUB datasets.

Calibration Deep neural networks tend to predict overconfidently (Thulasidasan et al. 2019). However, mixup methods can alleviate this problem. To show the generality of AutoMix, the mixup algorithms are evaluated on the expected calibration error (ECE) (Guo et al. 2017) on CIFAR-100, i.e., the absolute discrepancy between accuracy and confidence. As shown in Fig.6, AutoMix has the best calibration effect among all competitors, closest to the red diagonal. We can see from the figure that the Cut series does not well on calibration, but may further aggravate the overconfidence; while Input and Manifold mixup calibrate the predictions, but makes the model have the tendency of under-confidence.

Robustness Against Corruption AugMix (Hendrycks et al. 2019) is proposed to improve robustness against natural corrupted data by performing mixup between clean and corrupted images. AugMix employs Jensen-Shannon divergence (JSD) between network outputs of a clean image and two AugMix images as a consistency loss. However, the improvement of AugMix is very limited on clean data.

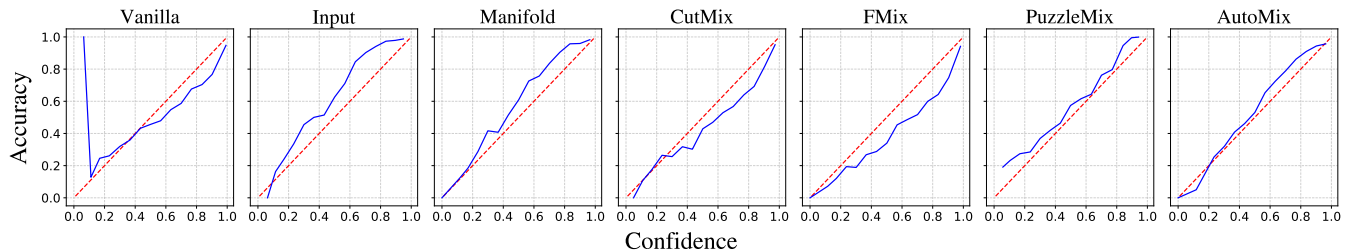


Figure 6: Calibration plots of various mixup methods and AutoMix on CIFAR-100 using ResNet-18

We evaluated various methods on the test accuracy using both the CIFAR-100-C (Hendrycks and Dietterich 2019) and CIFAR-100 (clean) datasets. Notice that CIFAR-100-C is designed for evaluating the corruption robustness. The data is corrupted in 19 different ways, including noise, blur, weather, and digital corruption, etc. In Tab.2, the AutoMix shows a consistent top level in both clean and corruption data.

Dataset	Vanilla	Mixup	CutMix	PuzzleMix	AugMix	Ours
CIFAR-100	80.24	82.44	81.09	82.76	81.18	83.13
CIFAR-100-C	51.71	58.10	49.32	57.82	66.54	58.35

Table 2: Top-1 accuracy on CIFAR-100 (clean) and CIFAR-100-C (corruption) based on ResNeXt-50 (32x4d).

ImageNet Datasets

Settings. In the large data scenario, which is a general challenging task for mixup methods, we evaluate the AutoMix on ImageNet-1k and Tiny-ImageNet benchmarks. The standard augmentations `RandomResizedCrop` and `RandomFlip` are used for all mixup algorithms by default. SGD weight decay parameter is set to 0.0001, momentum parameter is set to 0.9. On ImageNet, the initial learning rate is set to 0.1, batch size is set to 256, and the total epochs is 300. On Tiny-ImageNet, we trained for 400 epochs with the initial learning rate is 0.2 and the batch size is set to 100.

Method	Tiny ImageNet		ImageNet-1k			
	R-18	RX-50	R-18	R-34	R-50	R-101
Vanilla	61.68	65.04	71.83	75.29	77.35	78.91
MixUp	63.39	66.36	71.72	75.73	78.44	80.60
CutMix	64.40	66.47	70.03	75.16	78.69	80.59
ManifoldMix	62.76	67.30	71.73	75.44	78.21	80.64
SaliencyMix	64.95	66.55	70.21	75.01	78.46	80.45
FMix	62.28	65.08	70.30	75.12	78.51	80.20
PuzzleMix	65.63	66.92	71.64	75.84	78.87	80.67
ResizeMix	64.50	65.87	71.32	75.64	78.91	80.52
AutoMix (Ours)	67.33	70.72	72.05	76.10	79.25	80.98
Gain	+2.30	+3.42	+0.22	+0.26	+0.34	+0.31

Table 3: Top-1 accuracy on Tiny ImageNet and ImageNet-1k dataset based on various network architectures.

Classification. The top-1 accuracy on the Tiny-ImageNet and ImageNet is reported in Tab.3. It shows that AutoMix outperforms other methods on the Top-1 classification accuracy in both datasets, especially on the Tiny-ImageNet dataset, whose margin surpasses the existing best algorithm by 2.30% and 3.42% on ResNet-18 and ResNeXt-50, separately. On the ImageNet dataset, an anomaly can be noted that when training based on the lightweight backbone networks ResNet-18 (R-18) and ResNet-34 (R-34), *it is hard for the previous algorithms to achieve as high accuracy as Vanilla*. This result indicates that the offline approaches increase the difficulty of network optimization in the lightweight scenarios on large scale dataset. *On the contrary, our approach achieves stable performance gains on both different scale backbones.*

5.2 Fine-grained Dataset

We follow transfer learning settings on CUB-200 and follow the standard augmentation settings as in Sec.5.1. We use

the pretrained model provided on the Pytorch website as initialization, and set the initial learning rate to 0.001, the batch size is 16, and trained for 200 epochs.

Fine-grained classification. Tab.1 demonstrates AutoMix achieves best performance in fine-grained scenarios, which verifies that AutoMix has flexible adaptability to fine-grained settings. we improved the Vanilla by 2.19% and 3.55% on the CUB-200 based on ResNet-18 and ResNeXt-50, respectively.

Localization. Weakly supervised object localization (WSOL) aims to localize objects of interests without bounding boxes given. We test the WSOL performance of various algorithms trained on CUB-200. We use CAM (Selvaraju et al. 2019) with a threshold $\delta \in \{0.3, 0.5, 0.7\}$ as a supervision signal and follow MaxBoxAccV2 protocol (Choe et al. 2020). Tab.4 demonstrate our approach is the best to localize semantic regions.

Backbone	Vanilla	Mixup	CutMix	FMix	PuzzleMix	Ours
R-18	46.62	46.62	44.85	47.30	47.95	48.46
RX-50	47.28	48.32	47.12	49.20	48.34	50.10

Table 4: MaxBoxAcc for the WSOL task on CUB-200 based on ResNet-18 and ResNeXt-50 (32x4d).

5.3 Ablation Study

In this section, ablation studies are performed on image classification datasets. At first, Sec.5.3 analyzes the effectiveness of the MP, MB \mathcal{M}_ϕ , and CE loss on CIFAR-100 dataset and Tiny-ImageNet; Sec.5.3 analyzes the impact of the hyperparameter configurations on the performance of AutoMix on CIFAR-100. At last, we demonstrated the cost of selecting different feature layer and also compared the training computational complexity with other counterparts in Sec.5.4.

Effectiveness Analysis We first specifically analyzes the effectiveness of the proposed momentum pipeline (MP) and Mix Block \mathcal{M}_ϕ . In this experiment, MP is equipped on the Input MixUp, CutMix and \mathcal{M}_ϕ . We report the Top-1 classification accuracy of each combination on the CIFAR-100 and Tiny-ImageNet dataset based on ResNet-18 with training for 800 epochs. The hyperparameters are consistent with the previous configuration. In Tab.6, on both datasets, we can see the importance of MP because the performance of module \mathcal{M}_ϕ is 2.69% and 3.18% lower without using MP. Besides, recalling the results shown in Fig.5, MP is a general pipeline which can significantly accelerate the convergence speed and training stability of the mixup training, especially on AutoMix. In addition, the use of CE loss also has gain for our algorithm, but it has very limited effect on the other mixup algorithms. We then analyze the proposed mask loss \mathcal{L}_{mask} with L_1 and L_2 -norm, as shown in Tab.5. It shows that L_1 -norm with $\epsilon = 0.1$ achieves the best performance.

Effect of hyperparameters In this subsection, we discuss the effect of each hyperparameter on the classification performance. The settings of following experiments refer to Sec.5. In AutoMix, the stem structure of ResNet is skipped, and we only use the feature maps output from the first four bottleneck

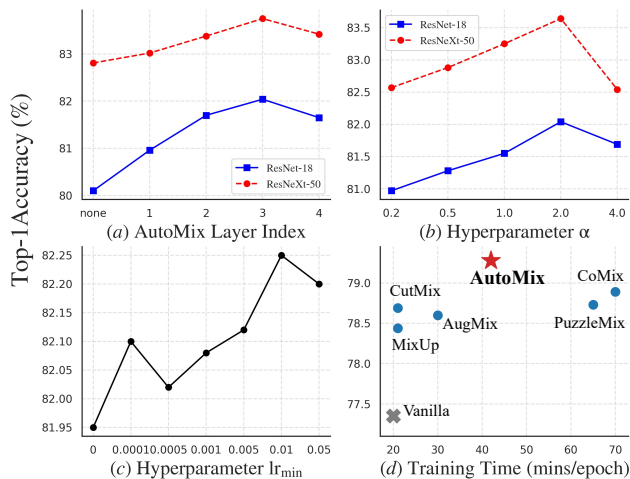


Figure 7: Ablation of AutoMix (a) layer depth l , (b) α , and (c) lr_{min} on CIFAR-100 of top-1 accuracy. (d) top-1 accuracy and the training time on ImageNet-1k of various methods based on ResNet-50 with 100-epoch training.

modules, where l_1 to l_4 represent the C1 to C4 bottleneck modules, respectively. The results are shown in Fig.7.

Backbone	(none)	L_1 ($\epsilon = 0$)	L_1 ($\epsilon = 0.1$)	L_1 ($\epsilon = 0.2$)	L_2 ($\epsilon = 0.1$)
R18	67.21	67.36	67.33	67.29	67.30
RX50	69.85	70.21	70.72	70.04	70.56

Table 5: Ablation of the mask loss \mathcal{L}_{mask} on Tiny-ImageNet based on ResNet-18 and ResNeXt-50 (32x4d).

modules	CIFAR-100			Tiny-ImageNet		
	MixUp	CutMix	\mathcal{M}_ϕ	MixUp	CutMix	\mathcal{M}_ϕ
(none)	79.12	78.17	78.45	63.39	64.40	63.49
+CE	80.30	78.25	79.23	64.05	64.34	63.07
+MP	80.82	79.54	81.14	66.02	65.72	66.67
+MP+CE	80.21	79.56	81.23	66.10	64.95	66.89

Table 6: Ablation study of the MP and the cross-entropy loss \mathcal{L}_{CE} on CIFAR-100 and Tiny-ImageNet based on ResNet-18.

Feature layers. We test the performance of using different feature layers based on two ResNet backbones four datasets, the results is shown in Fig.7 (a). AutoMix achieves best accuracy when using feature layer L_3 , while the performance when using shallower feature layer is poorer. The main reason is that features in this layer have both higher spatial resolution and rich semantic information, which facilitates the module \mathcal{M}_ϕ to predict the semantic share of each of the two input features on each image and represent class-related information more finely as sample mixture masks.

Alpha. Based on feature layer L_3 , the ablation study was continued for $\alpha \in \{0.2, 0.5, 1.0, 2.0, 4.0\}$, experiments results are presented in Fig.7 (b). It is clear that AutoMix reaches best performance when $\alpha = 2$. This phenomenon may be implied that a larger ratio of mixing is preferred during the training process by the module \mathcal{M}_ϕ online learning mixing strategy. The distribution in $Beta$ is concave when

$\alpha < 1$, approximates a Gaussian distribution when $\alpha \geq 2$, and has a higher probability of mixed ratio λ around 0.5. Therefore, $\alpha = 2$ can generate more mixed samples which helps with online learning mixup strategies.

Besides, AutoMix performs better when using higher lr_{min} . In general, lr_{min} can be adjusted according to the initialized learning rate r , which is usually taken as $lr_{min} = \frac{1}{10}lr_{base}$, which will make the encoder k to be trained fully, the ablation results are shown in Fig.7 (c).

5.4 Computational Complexity

Parameters of layers Based on R-18 and RX-50, we calculated the number of parameters (#params) and the training time (mins per epoch) of AutoMix under different feature layers as the MB input on CIFAR dataset. Generally, we choose layer 3 (l_3) as the default setting. The parameter increment brought by AutoMix w.r.t. the number of parameters of R-18 and RX-50 is only 0.015% and 0.062%. As the layer deepens, the deeper features have lower spatial resolution and richer semantic information, ensuring higher computational efficiency for the MB to model pair-wise cross-attention.

Backbone	Vanilla	AutoMix l_1	AutoMix l_2	AutoMix l_3	AutoMix l_4
R-18	11.27M 3mins	11.38M 10mins	11.39M 6mins	11.44M 5mins	11.64M 4mins
RX-50	23.38M 17mins	23.80M 62mins	23.86M 38mins	24.84M 28mins	27.99M 26mins

Table 7: Number of parameters and training time (mins/epoch) of choosing different feature layer l on Tiny ImageNet.

Efficiency of algorithms In Fig.7 (d), we further counted the training time and top-1 classification accuracy of various methods on ImageNet-1k with 100-epoch training. Although handcrafted mixup methods have a small extra computational overhead compared to vanilla, their performance improvements are also limited. In contrast, saliency-based methods, such as PuzzleMix, need extensive extra time to compute the saliency region to optimize the mixup policy offline, and their running times are usually three times slower than the vanilla. However, AutoMix is directly supervised by classification losses for generating mixed samples online and performing mixup classification, which takes advantage of the computational efficiency of neural networks and saves extra time for computing saliency (such as gradCAM). In a word, AutoMix is stable and significantly improves overall performance.

6 Conclusion

In this paper, we propose a *AutoMix* framework, which optimizes both the mixed sample generation task and the mixup classification task in a momentum training pipeline. Without adding cost to inference, AutoMix can generate out-of-manifold samples with adaptive masks. Extensive experiments have shown the effectiveness and excellent generalizability of the proposed AutoMix on CIFAR, ImageNet, and CUB-200 datasets. On top of that, we also outperformed other Mixup algorithms when transferring the pretrained model to detection tasks as well. Furthermore, the proposed momentum training pipeline serves a significant improvement in convergence speed and overall performance.

References

- Baek, K.; Bang, D.; and Shim, H. 2021. GridMix: Strong regularization through local context mapping. *Pattern Recognition*, 109.
- Ben-David, S.; Blitzer, J.; Crammer, K.; Kulesza, A.; Pereira, F.; and Vaughan, J. W. 2010. A theory of learning from different domains. *Machine learning*, 79(1): 151–175.
- Bishop, C. M. 2006. *Pattern recognition and machine learning*. Springer.
- Chen, L.-C.; Papandreou, G.; Kokkinos, I.; Murphy, K.; and Yuille, A. L. 2017. Deeplab: Semantic image segmentation with deep convolutional nets, atrous convolution, and fully connected crfs. *IEEE transactions on pattern analysis and machine intelligence*, 40(4): 834–848.
- Choe, J.; Oh, S. J.; Lee, S.; Chun, S.; Akata, Z.; and Shim, H. 2020. Evaluating weakly supervised object localization methods right. In *Proceedings of the IEEE/CVF Conference on Computer Vision and Pattern Recognition*, 3133–3142.
- Chrabaszcz, P.; Loshchilov, I.; and Hutter, F. 2017. A down-sampled variant of imagenet as an alternative to the cifar datasets. *arXiv preprint arXiv:1707.08819*.
- Devlin, J.; Chang, M.-W.; Lee, K.; and Toutanova, K. 2018. Bert: Pre-training of deep bidirectional transformers for language understanding. *arXiv preprint arXiv:1810.04805*.
- Faramarzi, M.; Amini, M.; Badrinaaraayanan, A.; Verma, V.; and Chandar, S. 2020. PatchUp: A Regularization Technique for Convolutional Neural Networks. *arXiv preprint arXiv:2006.07794*.
- Grill, J.-B.; Strub, F.; Althé, F.; Tallec, C.; Richemond, P. H.; Buchatskaya, E.; Doersch, C.; Pires, B. A.; Guo, Z. D.; Azar, M. G.; et al. 2020. Bootstrap your own latent: A new approach to self-supervised learning. *arXiv preprint arXiv:2006.07733*.
- Guo, C.; Pleiss, G.; Sun, Y.; and Weinberger, K. Q. 2017. On calibration of modern neural networks. In *International Conference on Machine Learning*, 1321–1330. PMLR.
- Harris, E.; Marcu, A.; Painter, M.; Niranjana, M.; and Hare, A. P.-B. J. 2020. Fmix: Enhancing mixed sample data augmentation. *arXiv preprint arXiv:2002.12047*, 2(3): 4.
- He, K.; Fan, H.; Wu, Y.; Xie, S.; and Girshick, R. 2020. Momentum contrast for unsupervised visual representation learning. In *Proceedings of the IEEE/CVF Conference on Computer Vision and Pattern Recognition*, 9729–9738.
- He, K.; Zhang, X.; Ren, S.; and Sun, J. 2016. Deep residual learning for image recognition. In *Proceedings of the IEEE conference on computer vision and pattern recognition*, 770–778.
- Hendrycks, D.; and Dietterich, T. 2019. Benchmarking neural network robustness to common corruptions and perturbations. *arXiv preprint arXiv:1903.12261*.
- Hendrycks, D.; Mu, N.; Cubuk, E. D.; Zoph, B.; Gilmer, J.; and Lakshminarayanan, B. 2019. Augmix: A simple data processing method to improve robustness and uncertainty. *arXiv preprint arXiv:1912.02781*.
- Kim, J.-H.; Choo, W.; Jeong, H.; and Song, H. O. 2021. Co-Mixup: Saliency Guided Joint Mixup with Supermodular Diversity. *arXiv preprint arXiv:2102.03065*.
- Kim, J.-H.; Choo, W.; and Song, H. O. 2020. Puzzle mix: Exploiting saliency and local statistics for optimal mixup. In *International Conference on Machine Learning*, 5275–5285. PMLR.
- Krizhevsky, A.; Hinton, G.; et al. 2009. Learning multiple layers of features from tiny images.
- Lin, T.-Y.; Goyal, P.; Girshick, R.; He, K.; and Dollár, P. 2017. Focal loss for dense object detection. In *Proceedings of the IEEE international conference on computer vision*, 2980–2988.
- Loshchilov, I.; and Hutter, F. 2016. Sgdr: Stochastic gradient descent with warm restarts. *arXiv preprint arXiv:1608.03983*.
- Qin, J.; Fang, J.; Zhang, Q.; Liu, W.; Wang, X.; and Wang, X. 2020. ResizeMix: Mixing Data with Preserved Object Information and True Labels. *arXiv preprint arXiv:2012.11101*.
- Ren, S.; He, K.; Girshick, R.; and Sun, J. 2015. Faster r-cnn: Towards real-time object detection with region proposal networks. *arXiv preprint arXiv:1506.01497*.
- Ronneberger, O.; Fischer, P.; and Brox, T. 2015. U-net: Convolutional networks for biomedical image segmentation. In *International Conference on Medical image computing and computer-assisted intervention*, 234–241. Springer.
- Russakovsky, O.; Deng, J.; Su, H.; Krause, J.; Satheesh, S.; Ma, S.; Huang, Z.; Karpathy, A.; Khosla, A.; Bernstein, M.; et al. 2015. Imagenet large scale visual recognition challenge. In *International journal of computer vision*, 211–252. Springer.
- Selvaraju, R. R.; Cogswell, M.; Das, A.; Vedantam, R.; Parikh, D.; and Batra, D. 2019. Grad-CAM: Visual Explanations from Deep Networks via Gradient-based Localization. *arXiv preprint arXiv:1610.02391*.
- Silver, D.; Huang, A.; Maddison, C. J.; Guez, A.; Sifre, L.; Van Den Driessche, G.; Schrittwieser, J.; Antonoglou, I.; Panneershelvam, V.; Lanctot, M.; et al. 2016. Mastering the game of Go with deep neural networks and tree search. *nature*, 529(7587): 484–489.
- Srivastava, N.; Hinton, G.; Krizhevsky, A.; Sutskever, I.; and Salakhutdinov, R. 2014. Dropout: a simple way to prevent neural networks from overfitting. *The journal of machine learning research*, 15(1): 1929–1958.
- Thulasidasan, S.; Chennupati, G.; Bilmes, J.; Bhattacharya, T.; and Michalak, S. 2019. On Mixup Training: Improved Calibration and Predictive Uncertainty for Deep Neural Networks. *arXiv preprint arXiv:1905.11001*.
- Uddin, A.; Monira, M.; Shin, W.; Chung, T.; Bae, S.-H.; et al. 2020. SaliencyMix: A Saliency Guided Data Augmentation Strategy for Better Regularization. *arXiv preprint arXiv:2006.01791*.
- Verma, V.; Lamb, A.; Beckham, C.; Najafi, A.; Mitliagkas, I.; Lopez-Paz, D.; and Bengio, Y. 2019. Manifold mixup: Better representations by interpolating hidden states. In *International Conference on Machine Learning*, 6438–6447. PMLR.

Wah, C.; Branson, S.; Welinder, P.; Perona, P.; and Belongie, S. 2011. The caltech-ucsd birds-200-2011 dataset. California Institute of Technology.

Xie, S.; Girshick, R.; Dollár, P.; Tu, Z.; and He, K. 2017. Aggregated residual transformations for deep neural networks. In *Proceedings of the IEEE conference on computer vision and pattern recognition*, 1492–1500.

Yun, S.; Han, D.; Oh, S. J.; Chun, S.; Choe, J.; and Yoo, Y. 2019. Cutmix: Regularization strategy to train strong classifiers with localizable features. In *Proceedings of the IEEE/CVF International Conference on Computer Vision*, 6023–6032.

Zhang, H.; Cisse, M.; Dauphin, Y. N.; and Lopez-Paz, D. 2017. mixup: Beyond empirical risk minimization. *arXiv preprint arXiv:1710.09412*.

A Appendix

A.1 More Experiments and Ablations

We also evaluated AutoMix on another popular dataset named FGVC-Aircraft. The top-1 accuracy comparison with other methods is listed in Tab.8. Similarly, AutoMix surpasses its competitors by a large margin on R-18. Although the margin is dropped, our method still have the best performance.

Method	FGVC-Aircraft	
	R-18	RX-50
Vanilla	80.23	85.10
MixUp	79.52	85.18
CutMix	78.84	84.55
ManifoldMix	80.68	86.60
SaliencyMix	80.02	84.31
FMix	79.36	84.85
PuzzleMix	80.76	86.23
ResizeMix	78.10	84.08
AutoMix	81.37	86.69
Gain	+0.61	+0.09

Table 8: Top-1 accuracy of various algorithms based on ResNet-18 and ResNeXt-50 (32x4d) on CIFAR-100, CUB and FGVC-Aircraft datasets.

To demonstrate the robustness of our hyper-parameter, the extra ablation studies are conducted on various dataset, Tiny-ImageNet and ImageNet. As the same conclusion we have in the main body of this paper, the result in Fig.8 also recommend the choice of α is 2 and l is 3-th.

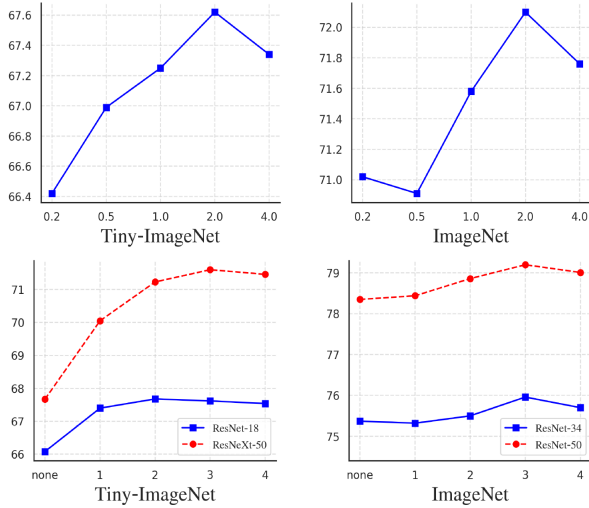


Figure 8: Top-1 accuracy ablation study on α value and feature layer l are shown at the top and bottom respectively.

A.2 Architecture of Network

The detailed structure of AutoMix is illustrated in Fig.9. Similar to the flow chat in the method, the module colored as blue can be updated by back propogation but not green. And the dotted line means stop-gradient.

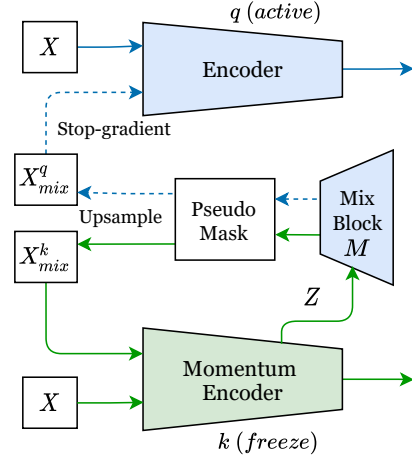


Figure 9: The network architecture of AutoMix.

A.3 Algorithm

We provide the pseudo code of AutoMix in Pytorch style:

Algorithm 1: Pseudocode AutoMix in Pytorch style.

```

1 # f_q, f_k, M: encoder networks and mix block
2 # lam_q, lam_k: sampled from Beta distribution
3 # idx_q, idx_k: rearrange index
4 # m: momentum coefficient
5
6 f_k.params = f_q.params # initialize
7
8 for x, y in loader: # load a minibatch
9     # two different permutation of data and label
10    x_q, x_k = x[idx_q], x[idx_k]
11    y_q, y_k = y[idx_q], y[idx_k]
12
13    # hidden representation and logits: NxCxWxH
14    lat_f = f_k(x)
15
16    # generate mixing sample, no gradient to q
17    m_q, m_k = M(x, [lam_q, lam_k], [idx_q, idx_k], lat_f)
18
19    # mixed and cls logits: NxC
20    logits_mix_k = f_k(m_k)
21    logits_cls_q, logits_mix_q = f_q(x), f_q(m_q)
22
23    # cross entropy losses for q and M
24    loss_cls_q = CELoss(logits_cls_q, y)
25    loss_mix_q = MCELoss(lam_q, logits_mix_q, y)
26    # loss_mask is computed in MCELoss for M
27    loss_mix_k = MCELoss(lam_k, logits_mix_k, y)
28    loss = loss_cls_q + loss_mix_q + loss_mix_k
29
30    # SGD update (q and M)
31    loss.backward()
32    update(f_q.params)
33    update(M.params)
34
35    # momentum update
36    f_k_params = m*f_k + (1-m)*f_q.params

```

A.4 Visualization on ImageNet



Figure 10: The upper part presents a visualization of the plot for a given $\lambda = 0.5$; and the lower presents the mixed samples when different λ values are taken.

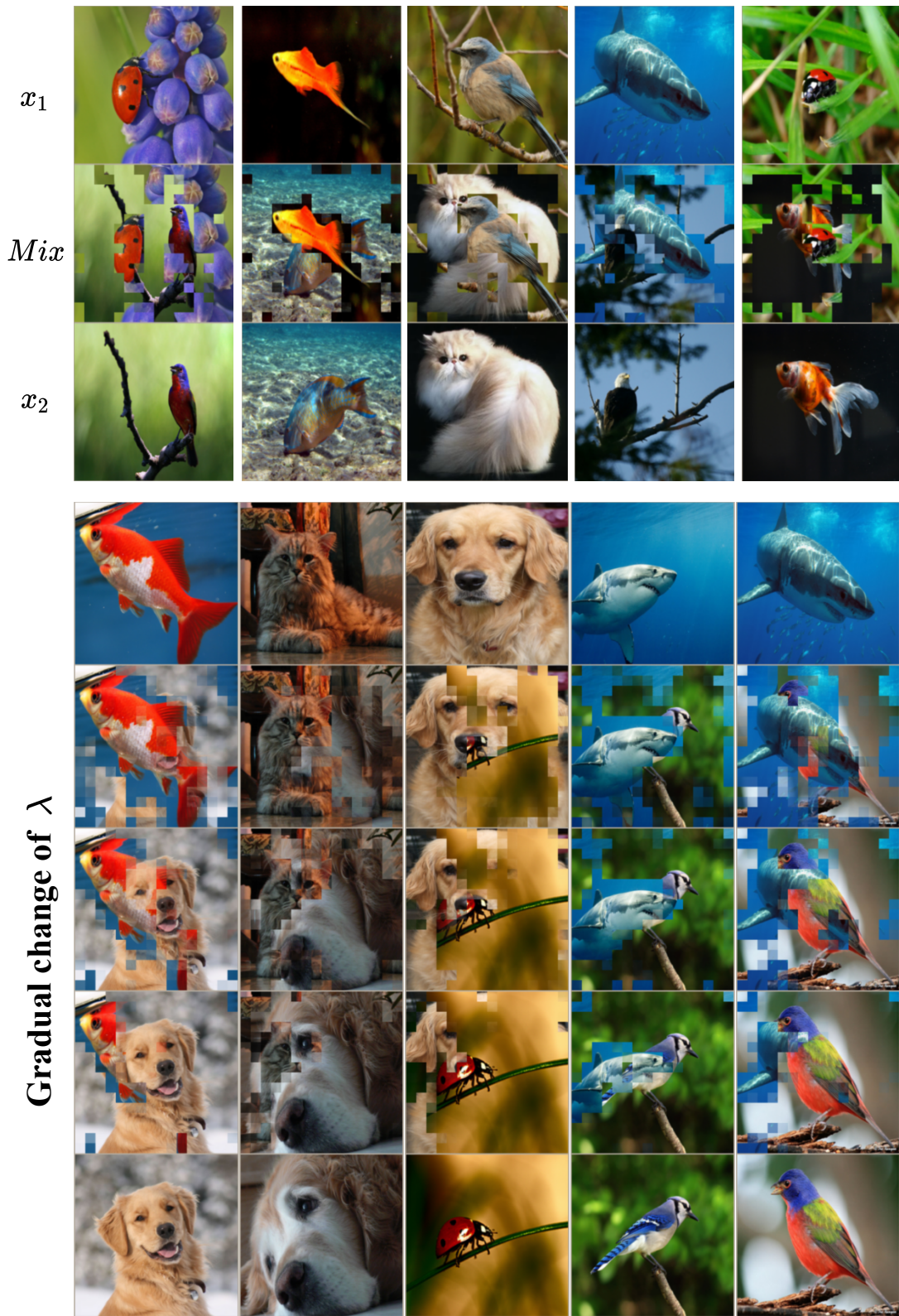


Figure 11: The upper part presents a visualization of the plot for a given $\lambda = 0.5$; and the lower presents the mixed samples when different λ values are taken.